

Interactions of Mono- and Divalent Metal Ions with Aspartic and Glutamic Acid Investigated with IR Photodissociation Spectroscopy and Theory

Jeremy T. O'Brien,[†] James S. Prell,[†] Jeff D. Steill,[‡] Jos Oomens,[‡] and Evan R. Williams^{*,†}

Department of Chemistry, University of California, Berkeley, California 94720-1460, and FOM Institute for Plasma Physics "Rijnhuizen", Edisonbaan 14, 3439 MN Nieuwegein, The Netherlands

Received: July 1, 2008; Revised Manuscript Received: August 8, 2008

The interaction of metal ions with aspartic (Asp) and glutamic (Glu) acid and the role of gas-phase acidity on zwitterionic stability were investigated using infrared photodissociation spectroscopy in the spectral range 950–1900 cm^{-1} and by hybrid density functional theory. Lithium ions interact with both carbonyl oxygen atoms and the amine nitrogen for both amino acids, whereas cesium interacts with both of the oxygen atoms of the C-terminus and the carbonyl oxygen of the side chain for Asp. For Glu, this structure is competitive, but a structure in which the cesium ion interacts with just the carbonyl oxygen atoms is favored and the calculated spectrum for this structure is more consistent with the experimentally measured spectrum. In complexes with either of these metal ions, both amino acids are non-zwitterionic. In contrast, $\text{Glu}\cdot\text{Ca}^{2+}$ and $\text{Glu}\cdot\text{Ba}^{2+}$ both adopt structures in which Glu is zwitterionic and the metal ion interacts with both oxygens of the C-terminal carboxylate and the carbonyl oxygen in the side chain. Assignment of the zwitterionic form of Glu is strengthened by comparisons to the spectrum of the protonated form, which indicate spectral features associated with a protonated amino nitrogen. Comparisons with results for glutamine, which adopts nearly the same structures with these metal ions, indicate that the lower ΔH_{acid} of Asp and Glu relative to other amino acids does not result in greater relative stability of the zwitterionic form, a result that is directly attributed to effects of the metal ions which disrupt the strong interaction between the carboxylic acid groups in the isolated, deprotonated forms of these amino acids.

Introduction

Metal ions and solvent molecules play important roles in the structure and reactivity of biomolecules.^{1,2} Many proteins require metal ions to fold and become active. Ion–protein interactions are involved in ion transport through cell membranes and in enzymatic catalysis of red-ox reactions. Competitive effects of solvent influence the interactions of metal ions with biomolecules. In the late 1800s, it was recognized that ions varied in their effects on fundamental properties of ionic solutions, such as their ability to denature proteins. Hofmeister ordered ions in their tendency to precipitate proteins or denature proteins,² and even today, the origin of this Hofmeister effect is still debated.^{3–5}

With mass spectrometry, it is possible to isolate and investigate the structures of cationized biomolecules^{6–50} and investigate how ions and water molecules competitively interact with biomolecules.^{18,22,47–49} Such experiments make possible a detailed understanding of competitive effects of ion and solvent interactions with biomolecules. Of particular interest to many groups has been the interaction of metal ions with amino acids and the effects of metal ions on the stability of the zwitterionic form of the amino acid.^{10–32,35,46–56} In isolation, all naturally occurring amino acids are non-zwitterionic, even the most basic amino acid, arginine, for which the zwitterionic structure is only 12–16 kJ/mol higher in energy.^{57–59} The zwitterionic form of an amino acid can be stabilized when a metal ion is attached.^{11–32,50–56} The zwitterionic form of arginine, in which

the side-chain guanidinium group is protonated and the C-terminus is deprotonated, is most stable when complexed to sodium and the larger alkali metal ions,^{11,17,50} and the zwitterionic forms of other amino acids have been reported for both mono-^{19,27} and dications.^{14,16,32,53–56}

Either increasing the proton affinity of the proton accepting site^{23–25,28,46,60,61} or increasing the acidity of the proton-donating group⁶⁰ can potentially stabilize the zwitterionic form of a molecule. For example, the stabilities of the zwitterionic forms of amino acids with aliphatic side chains when complexed with sodium ions are directly related to the proton affinity of the amino acid.^{23,24} For amino acids that have one or more heteroatoms in their side chain, such as basic or acidic amino acids, the relation can be much less direct.^{11–13,17,28,30,58,59} For example, the charge-solvated forms of lithiated arginine^{11,17} and lithiated glycine^{52,53} in which the amino acids are non-zwitterionic are both ~ 16 kJ/mol more stable than the corresponding zwitterionic forms despite the fact that the proton affinity of arginine is 160 kJ/mol higher than that of glycine.⁶² Heteroatoms in the side chain can result in significant stabilization of the charge-solvated structures.^{11–13,17,28,30,58,59} The roles of metal ion size, charge state, and amino acid basicity on the propensity for zwitterion formation have been extensively studied.^{11–32,46,52–56} In contrast, the role of gas-phase acidity on amino acid zwitterionic stability is less well known.

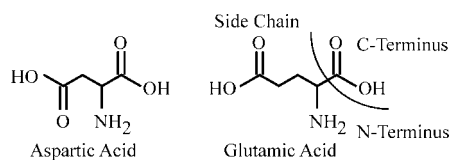
The gas-phase acidities (ΔH_{acid}) of the 20 naturally occurring α -amino acids range from ~ 1435 kJ/mol for glycine to ~ 1350 kJ/mol for aspartic (Asp) and glutamic (Glu) acid (Scheme 1), the two most acidic amino acids that have side-chain carboxylic acid groups.^{63,64} By comparison, the gas-phase acidity of propanoic acid ($\text{CH}_3\text{CH}_2\text{COOH}$) is ~ 1454 kJ/mol.⁶⁵ This indicates

* Address correspondence to this author. E-mail: williams@cchem.berkeley.edu, FAX: (510) 642-7714.

[†] University of California, Berkeley.

[‡] FOM Institute for Plasma Physics "Rijnhuizen".

SCHEME 1



that the intrinsic acidity of the C-terminus is higher than that of the side-chain carboxylic acid group, consistent with calculations which indicate that the C-terminus is preferentially deprotonated in the isolated amino acid.^{63,64} The high acidity of Asp and Glu can be attributed to the high stability of the deprotonated forms of these amino acids in which the hydrogen atom of the side-chain carboxylic acid interacts with the C-terminal carboxylate.^{63,64}

IR action spectroscopy can provide significant information about the structure of gas-phase ions and has been recently used to elucidate the structures of many cationized amino acids^{11–19,28–31,39} and amino acid complexes.^{34,35,40–45} Here, the results of IR action spectroscopy in the frequency range 950–1900 cm^{-1} and density functional theory calculations on $\text{Asp}\cdot\text{M}^+$, $\text{Glu}\cdot\text{M}^+$ ($\text{M} = \text{H}, \text{Li}, \text{and Cs}$), $\text{Glu}\cdot\text{Ca}^{2+}$, and $\text{Glu}\cdot\text{Ba}^{2+}$ are presented. From these results, information about the effects of mono- and divalent cations on the structures of Asp and Glu and the role of gas-phase acidity on zwitterion stability is obtained.

Experimental Section

IR Photodissociation Spectroscopy. All experiments were performed on a 4.7 T Fourier-transform ion cyclotron resonance mass spectrometer. The instrument⁶⁶ and experimental methods³¹ are described in detail elsewhere. In brief, cationized Asp and Glu were formed by electrospray ionization from a 60/40 water/methanol solution of 2 mM amino acid and 2 mM metal chloride salt infused at a rate of 15–20 $\mu\text{L}/\text{min}$. Precursor ions were mass-selected using stored waveform inverse Fourier transforms and subsequently irradiated for 2.5 to 4.5 s using tunable irradiation from the Free-Electron Laser for Infrared eXperiments (FELIX).⁶⁷ The same irradiation time was used for each ion and was selected based on the ion stability as indicated by photodissociation yield.

Computations. Low-energy structures of cationized Asp and Glu were generated using Monte Carlo conformational searching and the MMFFs force field as implemented in *Macromodel 9.1* (Schrödinger, Inc. Portland, OR). In the initial searches, no constraints were placed on the geometry, and 5000 conformers were generated for both non-zwitterionic and zwitterionic forms of $\text{Asp}\cdot\text{Li}^+$, $\text{Glu}\cdot\text{Li}^+$, $\text{Glu}\cdot\text{Ca}^{2+}$, and $\text{Glu}\cdot\text{Ba}^{2+}$. The resulting low-energy structures were sorted into different groups with similar metal coordination. Structures for cesiated complexes were generated by metal ion substitution into lithiated structures prior to geometry optimization. Representative structures from each group were geometry optimized in *Q-Chem v. 3.0*⁶⁸ using hybrid method density functional calculations (B3LYP) with the CRENLB⁶⁹ effective core potential for Cs, Ca, and Ba and the 6–31++G** basis set for all other atoms. Vibrational frequencies and intensities were calculated using the double harmonic approximation and the analytical Hessian of the energy-minimized structures using *Q-Chem v. 3.0*.⁶⁸ Most structures yielded all positive frequency vibrations, but two of structures for the cesiated species of non-zwitterionic (NZ) Asp and Glu each had two imaginary frequencies $<80 \text{ cm}^{-1}$ indicative of torsional modes on a very flat region of the

TABLE 1: Photodissociation Products of Protonated and Cationized Aspartic and Glutamic Acid

aspartic acid		glutamic acid	
cation	products (m/z)	cation	products (m/z)
H^+	$-\text{H}_2\text{O}$ (116) $-\text{formic acid}$ (88) $-\text{acetic acid}$ (74)	H^+	$-\text{H}_2\text{O}$ (130) $-\text{formic acid}$ (102) $-\text{H}_2\text{O}, \text{formic acid}$ (84)
Li^+	$\text{H}_2\text{CCHNH}_2\cdot\text{Li}^+$ (50) $\text{H}_2\text{NCH}_2\text{CHCO}\cdot\text{Li}^+$ (78) $-\text{formic acid}$ (94)	Li^+	$-\text{H}_2\text{O}$ (136) $-\text{formic acid}$ (108) $-\text{H}_2\text{O}, \text{formic acid}$ (90)
Cs^+	Cs^+ (133)	Cs^+	Cs^+ (133)
		Ca^+	$-\text{formic acid}$ (70.5) CaOH^+ (57) H_2NCO^+ (44)
		Ba^+	BaOH^+ (155) $-\text{H}_2\text{O}$ (133.5) $-\text{formic acid}$ (119.5) $-\text{BaOH}^+, \text{formic acid}$ (84)

potential energy surface or computational artifacts. In one of these structures, the cesium ion coordinates to the two carbonyl oxygen atoms (NZ $\text{O}_5\text{O}_\text{C}$; where S indicates the side-chain carbonyl oxygen atom and C indicates the C-terminal carbonyl oxygen atom). The other structure, NZ $\text{NO}_5\text{O}_\text{C}$, which results in imaginary frequencies is similar, except that the nitrogen of the N-terminus also solvates the cesium ion. Gibbs free energies including zero point energy corrections were determined at 0 and 298 K. All frequencies were scaled by 0.975. This scaling factor has been used previously in other IR studies in this region to compare experimental photodissociation spectra to spectra calculated at similar levels of theory as used in this study.^{13,14,28,29} The frequencies were convolved with a 40 cm^{-1} fwhm Lorentzian distribution, which provides a good fit to the observed peak shapes.

Results and Discussion

Photodissociation of protonated and metal cationized Asp and Glu results in dissociation by several different pathways that depend on the cation (Table 1). Rearrangement reactions resulting in loss of water or formic acid commonly occur. For both $\text{Asp}\cdot\text{Cs}^+$ and $\text{Glu}\cdot\text{Cs}^+$, bare cesium ion is the only product observed, consistent with a low binding energy for this large cation. For $\text{Glu}\cdot\text{Ca}^{2+}$ and $\text{Glu}\cdot\text{Ba}^{2+}$, both loss of formic acid and MOH^+ are observed. Photodissociation action spectra are obtained from the sum of the photodissociation product ion intensities divided by the total ion intensity measured as a function of photon energy. The laser power is relatively flat from 625 to 1250 cm^{-1} but decreases by $\sim 3\times$ between 1250 and 1900 cm^{-1} . To roughly account for this change in power, the action spectra are linearly power-corrected.³¹ The IR action spectra of $\text{Asp}\cdot\text{H}^+$, $\text{Asp}\cdot\text{Li}^+$, $\text{Asp}\cdot\text{Cs}^+$, $\text{Glu}\cdot\text{H}^+$, $\text{Glu}\cdot\text{Li}^+$, $\text{Glu}\cdot\text{Cs}^+$, $\text{Glu}\cdot\text{Ca}^{2+}$, and $\text{Glu}\cdot\text{Ba}^{2+}$ are shown in Figure 1. Information about the structure of these ions is obtained from comparison among the spectra reported here, comparison to previously reported IR action spectra of cationized amino acids,^{12–14,16,19,28–31} and comparison to calculated spectra of candidate low-energy structures. The relative Gibbs free energies of these low-energy structures at 0 and 298 K calculated at the B3LYP/CRENLB level of theory for Cs^+ , Ba^{2+} , and Ca^{2+} and B3LYP/6–31++G** for all other atoms are reported in Table 2.

There are a number of factors that can contribute to differences between IR photodissociation spectra and calculated absorption spectra. Band intensities are calculated using a double

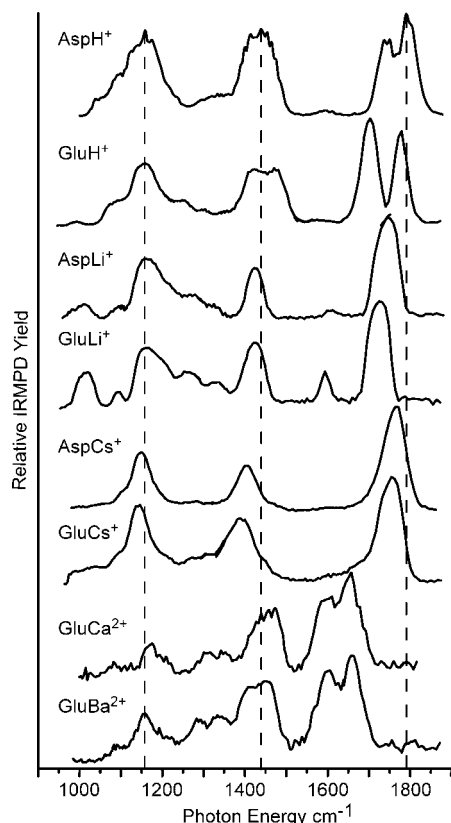


Figure 1. IRMPD action spectra of Asp•M⁺, Glu•M⁺, (M = H, Li, and Cs), Glu•Ca²⁺, and Glu•Ba²⁺.

TABLE 2: Relative Gibbs Free Energies at 0/298 K in kJ/mol Calculated with B3LYP Using CRENL Effective Core Potential for Cs, Ba, and Ca and 6-31++G for All Other Atoms**

structure	Asp•H ⁺	Glu•H ⁺
A	11/10	13/14
B	1/2	2/3
C	0/0	0/0
D	42/45	58/60

structure	Asp•Li ⁺	Glu•Li ⁺	Asp•Cs ⁺	Glu•Cs ⁺	Glu•Ca ²⁺	Glu•Ba ²⁺
NZ O _s OO _c			0/0	9/12		
NZ NO _s O _c	0/0	0/0	7/10	13/12	1/1	17/17
NZ O _s O _c	31/31	27/28	11/18	1/4	51/50	43/38
ZW OO _c	46/43	34/32	11/14	0/0	37/39	14/12
NZ OO _s			2/2	10/11		
ZW O _s OO _c					0/0	0/0

harmonic approximation which results in attendant uncertainties in comparing with measured spectra. IR photodissociation spectroscopy is a multiple photon process under these conditions.⁷⁰ The IR photodissociation spectrum of naphthalene cation is similar to the measured single-photon linear absorption spectrum.⁷¹ However, several factors can contribute to differences in spectra measured by the two methods. A more complete discussion of the dynamics of IRMPD in these experiments, and their effects on the resulting spectra are reviewed elsewhere.⁷⁰

Asp•H⁺ and Glu•H⁺. The IR action spectra of protonated Asp and Glu have many common features, including bands centered near 1790, 1710, 1600, 1450, 1300, and 1150 cm⁻¹ (Figure 2). In addition, the Glu•H⁺ spectrum contains two bands at 1250 and ~1000 cm⁻¹ that are not observed for Asp•H⁺. These additional bands are consistent with CH bending modes and C–C stretches associated with the additional CH₂ group in

the Glu side chain. The broad photodissociation intensity between 1375 and 1550 cm⁻¹ for Glu•H⁺ consists of two or more poorly resolved bands, whereas the feature for Asp•H⁺ is narrower, indicating closer spacing of these bands.

The bands in these spectra can be assigned to vibrational modes based on comparison to the previously reported spectra of protonated and metal cationized amino acids^{12–14,28–30} and to the calculated spectra of the lowest-energy structures for both Asp•H⁺ and Glu•H⁺ (Figure 2). These assignments are given in Table 3. The two peaks between 1700 and 1800 cm⁻¹ are consistent with carbonyl stretches. Carbonyl stretches of carboxylic acid groups have been reported previously in this spectral region for protonated arginine¹⁷ and lysine,²⁸ as well as for many metal-cationized amino acids.^{12,14,17,19,29–31}

Protonation at the N-terminus is at least 40 kJ/mol lower in energy than protonation at the carbonyl oxygen of the C-terminus (structures DI and DII, Figure 2). In all the low-energy structures, the protonated nitrogen donates one hydrogen bond to each of the carbonyl oxygen atoms. The H-bond distance to the side-chain and C-terminal carbonyl oxygens is ~1.5–1.6 Å and 2.1–2.2 Å, respectively, for these structures, consistent with a stronger hydrogen bond between the protonated N-terminus and the side-chain carbonyl oxygen. This strong hydrogen bond causes a significant red-shift in the carbonyl stretch of the side chain compared to that of the C-terminus. This red-shift is greater for Glu•H⁺ because the longer side chain provides greater flexibility, which enables formation of an even stronger ionic hydrogen bond between the protonated N-terminus and the carbonyl oxygen of the side chain.

The broad feature between 1375 and 1500 cm⁻¹ in the spectra of both Asp•H⁺ and Glu•H⁺ is consistent with previous assignments of hydrogen-bonded NH bends and CH bends.^{12–14,28–30} Below 1300 cm⁻¹, the most prominent feature in both IR action spectra is a peak centered around 1150 cm⁻¹. A similar band is observed for Gln•Li⁺, Lys•Li⁺, Ser•Li⁺, and Thr•Li⁺ and is assigned to the in-plane OH bend of the free hydrogen atom in a carboxylic acid group.^{12,13,28,30} For Asp•H⁺ and Glu•H⁺, both carboxylic acid groups contribute to this feature.

Calculated structures A and B are nearly identical except that, in structure A, the hydroxyl oxygen, instead of the carbonyl oxygen, of the C-terminal carboxylic acid group accepts the hydrogen bond. This interaction is less favorable, and structure A is 10 and 14 kJ/mol less stable than structure B for Asp•H⁺ and Glu•H⁺, respectively. The spacing between carbonyl oxygen stretches in the measured spectra is more consistent with structures B and C. Structures B and C are also very similar and have energies within 3 kJ/mol of each other. Their calculated IR spectra are consistent with the measured IR action spectra. Because these structures are nearly isoenergetic and almost certainly have very low barriers for interconversion, it is likely that both structures are populated and both contribute to the observed IR action spectra. The experimental spectra of Asp•H⁺ and Glu•H⁺ provide a model for spectroscopic features associated with a protonated N-terminus of Asp and Glu and can be used to identify expected spectral features in possible zwitterionic structures for metal-cationized Asp and Glu.

Asp•Li⁺ and Glu•Li⁺. The IR action spectra of Asp•Li⁺ and Glu•Li⁺ are also very similar to each other, but the relative intensities of some bands differ (Figure 3). The bands at ~1000 and ~1600 cm⁻¹ are substantially more intense in the Glu•Li⁺ spectrum, although these features are certainly present in the Asp•Li⁺ spectrum. Instead of two distinct bands corresponding to the two carbonyl stretches in the spectra of the protonated species, there is only a single band in the carbonyl stretch region

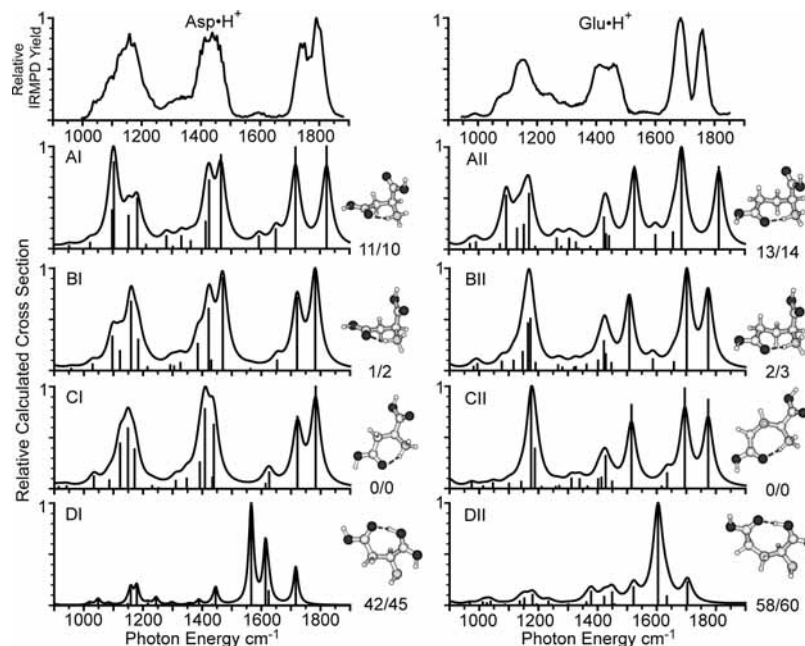


Figure 2. IRMPD action spectra of Asp•H⁺ (left) and Glu•H⁺ (right) obtained with 2.5 s laser irradiation and B3LYP/6-31++G** calculated spectra of candidate low-energy structures (frequencies scaled by 0.975). Energies are Gibbs free energies at 0 K/298 K in kJ/mol.

TABLE 3: IRMPD Band Assignments for Asp•H⁺

IRMPD freq. (cm ⁻¹)	assignment	structure CI calc. freq. (cm ⁻¹)
1789	COOH _C asym. stretch	1783
1744	COOH _S asym. stretch	1722
1593	NH ₃ scissor	1627
1370–1500	NH ₃ umbrella	1439
	NH ₃ umbrella/OH _S bend	1409
	OH _C bend/CH wag	1392
1050–1250	OH _S bend	1172
	OH _C bend	1149
	CH ₂ twist/OH _{C/S} bends	1122

of the lithiated species, indicating that the ionic hydrogen bonds that occur for the protonated amino acids are not present in the lithiated forms. A zwitterionic structure for the amino acid in the metal cationized species should have two distinguishable carbonyl stretch vibrations owing to the presence of both a carboxylate and a carboxylic acid, and can be ruled out based on the single, albeit broad, band in this region.

Three structural families were identified from conformational searching of the lithiated amino acids: a non-zwitterionic (NZ) structure where one oxygen from each of the carboxylic acid groups and the N-terminal nitrogen all coordinate to the metal ion (NZ NO_SO_C; where S indicates the side-chain carbonyl oxygen atom and C indicates the C-terminal carbonyl oxygen atom); an NZ O_SO_C coordinated structure in which the N-terminal nitrogen accepts a hydrogen bond donated by the backbone carboxylic acid group; and the lowest-energy zwitterionic (ZW) structure for both species, ZW OO_C, where the metal ion coordinates to both the oxygen atoms of the deprotonated C-terminus and the protonated N-terminus donates a hydrogen bond to an oxygen atom of the carboxylic acid and carboxylate groups. A similar ZW OO_C structure which instead has a deprotonated side chain was calculated to be ~6 kJ/mol less stable. This is consistent with the lower Δ*H*_{acid} of the C-terminus compared with that of the side chain for both amino acids.^{63,64}

The band observed in the experimental spectra at ~1600 cm⁻¹ is consistent with an NH₂ scissoring mode in both the NZ

NO_SO_C and NZ O_SO_C calculated spectra. The calculated intensity of this vibration is similar for both lithiated species, whereas this band is clearly more intense in the measured spectrum of Glu•Li⁺. The band at ~1000 cm⁻¹ is consistent with the out-of-plane wag of the NH₂ group in the NZ NO_SO_C calculated spectrum. This vibration for the NZ O_SO_C structure is calculated to occur at a substantially lower frequency, ~850 cm⁻¹. The relative Gibbs free energies at 298 K of the three calculated structures indicate that the NZ NO_SO_C structure is lowest in energy for both Asp•Li⁺ and Glu•Li⁺; the NZ O_SO_C structure is higher by 31 and 28 kJ/mol, respectively, and the zwitterionic structures are even higher. The relative intensities of the ~1000 cm⁻¹ band, the overall excellent agreement between the measured and calculated spectra, and the calculated relative energies all indicate that both Asp•Li⁺ and Glu•Li⁺ adopt an NZ NO_SO_C coordinated structure similar to the lowest-energy structures reported for lithiated glutamine,¹³ serine,¹² and threonine,³⁰ which also have oxygen atom containing side chains.

Asp•Cs⁺ and Glu•Cs⁺. The IR action spectra of Asp•Cs⁺ and Glu•Cs⁺ are very similar to each other and consist of three distinct, broad bands centered at ~1760, 1400, and 1150 cm⁻¹ (Figure 4). These similar spectra indicate that the difference in the length of the side chain plays little role in the structure adopted by each amino acid when complexed with cesium. However, the calculated energies and spectra of candidate low-energy structures indicate that Asp•Cs⁺ and Glu•Cs⁺ adopt different structures, although the difference is very subtle. As was the case for lithium, the carbonyl stretches are not resolved, resulting in a relatively broad band at ~1760 cm⁻¹. This band is blue-shifted from the corresponding band in the lithiated spectra by ~20 cm⁻¹. A similar shift has been observed between the lithiated and cesiated IR action spectra of glutamine,¹³ tryptophan,²⁹ serine,¹² and threonine,³⁰ consistent with less transfer of electron density for the larger cation. As for the lithiated species, zwitterionic forms of the cesiated species should have two different carbonyl stretch features due to the presence of both a carboxylic acid and a carboxylate group and can be ruled out by the position of the single broad band in this

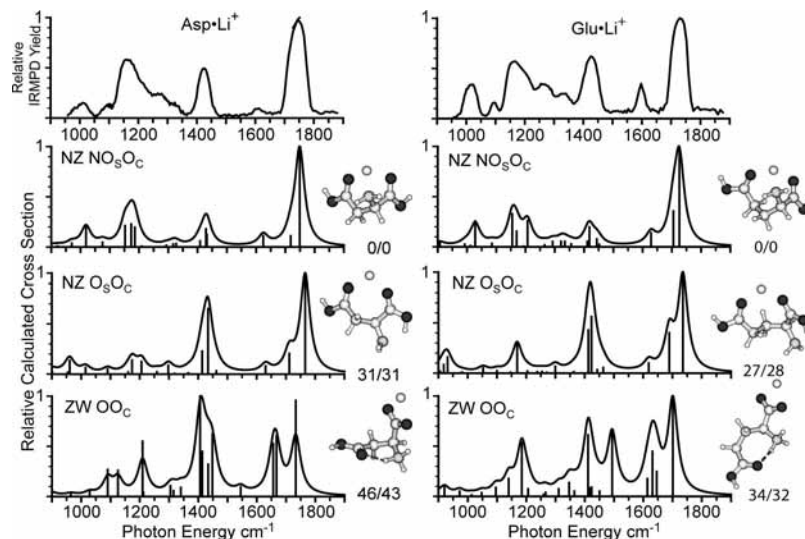


Figure 3. IRMPD action spectra of Asp•Li⁺ (left) and Glu•Li⁺ (right) obtained with 4.5 s laser irradiation and B3LYP/6-31++G** calculated spectra of candidate low-energy structures (frequencies scaled by 0.975). Calculated frequencies have been scaled by 0.975. Energies are Gibbs free energies at 0 K/298 K in kJ/mol.

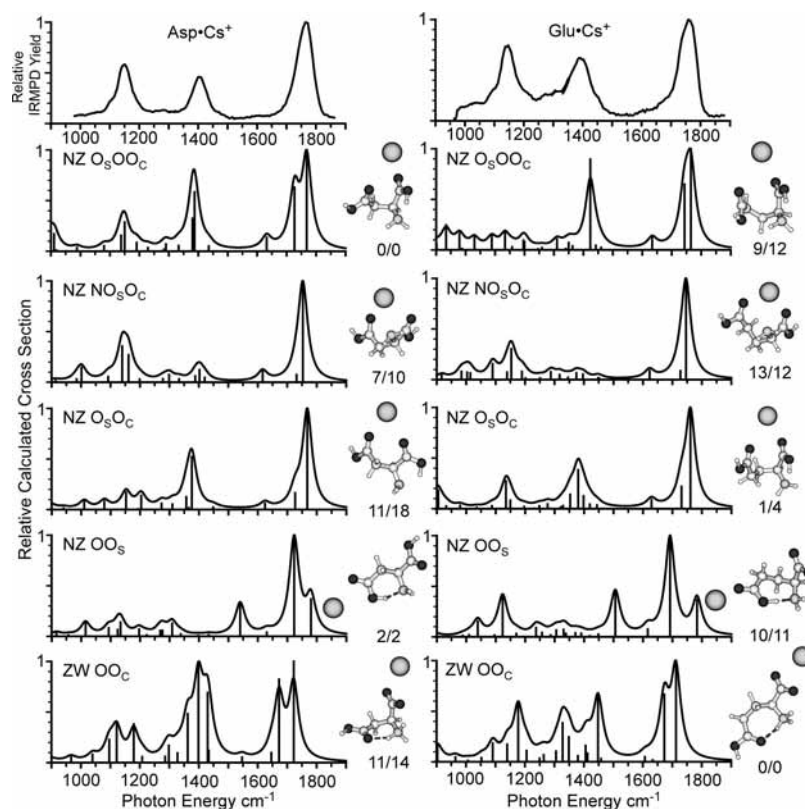


Figure 4. IRMPD action spectra of Asp•Cs⁺ (left) and Glu•Cs⁺ (right) obtained with 2.5 s laser irradiation and B3LYP/6-31++G** calculated spectra of candidate low-energy structures; the CRENNBL effective core potential was used for Cs⁺ (frequencies scaled by 0.975). Energies are Gibbs free energies at 0 K/298 K in kJ/mol.

region. In addition, the NH bending modes around 1400 cm⁻¹ in the spectra of the cesiated species do not match the features observed for the protonated species indicating that the N-terminus is not protonated and hence the cesiated amino acids are not zwitterionic.

The most apparent difference between the cesiated and lithiated IR action spectra is the absence of distinct bands at 1000 and 1600 cm⁻¹ in the spectra of the cesiated species, whereas these features are clearly present in the spectra of the lithiated species. These bands are consistent with NH bends of an amine coordinating with a metal ion (vide supra). The

absence of these bands in the Cs⁺ spectra indicates that the nitrogen is not coordinating directly to the cesium ion.

The same structural families identified for the lithiated species were also calculated to be stable for Cs⁺, but two additional conformational families were identified: an NZ O_sOO_e structure in which the cesium coordinates to both oxygens of the C-terminal carboxylic acid group and the side-chain carbonyl oxygen and an NZ OO_s structure in which the metal ion coordinates to both oxygens of the side-chain carboxylic acid that also donates a hydrogen bond to the N-terminus. The NZ O_sOO_e structure is calculated to be unstable for the lithiated

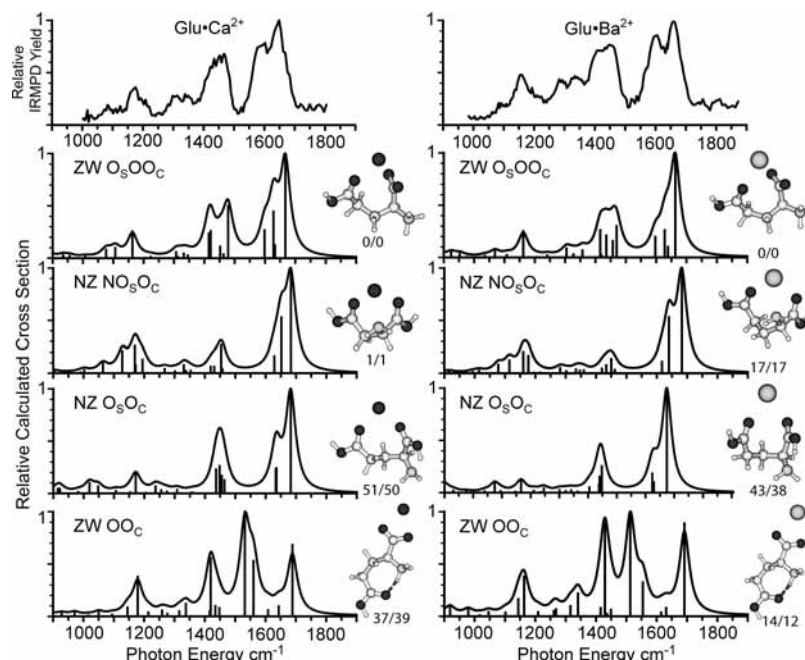


Figure 5. IRMPD action spectra of $\text{Glu}\cdot\text{Ca}^{2+}$ (left) and $\text{Glu}\cdot\text{Ba}^{2+}$ (right) obtained with 3.5 s laser irradiation and B3LYP/6-31++G** calculated spectra of candidate low-energy structures, the CRENLB effective core potential was used for Ba^{2+} (frequencies scaled by 0.975). Energies are Gibbs free energies at 0 K/298 K in kJ/mol.

species and isomerizes during energy minimization to an NZ O_5OC coordinated structure. The NZ O_5OOc structure is lowest in energy for $\text{Asp}\cdot\text{Cs}^+$, whereas the ZW OOc structure is calculated to be the most stable form of $\text{Glu}\cdot\text{Cs}^+$. However, the IR action spectrum shows no significant photodissociation indicative of the carbonyl stretch associated with a carboxylate group at 1675 cm^{-1} , and the experimental features below 1500 cm^{-1} do not match the calculated spectrum of the zwitterionic structure (Figure 4). For both Asp and Glu, a zwitterionic structure with a deprotonated side chain spontaneously transferred a proton from the protonated N-terminus to the side chain upon geometry optimization, resulting in a non-zwitterionic side-chain coordinated structure NZ OO_5 . The OH bend of the hydrogen-bonded side-chain carboxylic acid is calculated to occur at $\sim 1540\text{ cm}^{-1}$ with significant intensity. These NZ OO_5 structures can be ruled out by the absence of this feature in the IR action spectra and the absence of a strong band at $\sim 1400\text{ cm}^{-1}$ in the calculated spectra.

The NZ O_5OOc structure of $\text{Asp}\cdot\text{Cs}^+$ is calculated to have an intense band corresponding to the OH bend of the side-chain carboxylic acid at $\sim 1150\text{ cm}^{-1}$, whereas this feature is much weaker in the calculated spectrum of the NZ O_5Oc structure. The intensity of the experimentally observed dissociation at 1150 cm^{-1} is substantial and indicates the presence of NZ O_5OOc or NZ NO_5Oc structures for Asp. The absence of a distinct band at 1000 cm^{-1} , observed in the lithiated spectra and calculated NZ NO_5Oc structure, indicates that this structure is absent or contributes only minimally to the spectrum of $\text{Asp}\cdot\text{Cs}^+$. The calculated spectra contain an NH_2 scissoring mode at $\sim 1600\text{ cm}^{-1}$ for all three non-zwitterionic structures, suggesting that the out-of-plane NH_2 wag at 1000 cm^{-1} is more sensitive to metal ion coordination with the nitrogen. On the basis of these comparisons, the IR action spectrum is most consistent with an NZ O_5OOc structure, although contribution from NZ O_5Oc or NZ NO_5Oc structures cannot be ruled out.

For $\text{Glu}\cdot\text{Cs}^+$, the IR action spectrum is most consistent with the calculated spectrum of an NZ O_5Oc structure (Figure 4), which has three distinct bands centered at ~ 1760 , 1385 , and

1140 cm^{-1} that match very well with the observed bands. However, other structures may also be present. The NZ O_5Oc and NZ O_5OOc forms of $\text{Glu}\cdot\text{Cs}^+$ differ only by a small displacement of the large cesium cation and almost certainly have a low barrier to interconversion. Thus, both of these structures are likely present. The calculated spectrum of the NZ O_5OOc structure lacks a distinct peak at $\sim 1140\text{ cm}^{-1}$ because the OH bend which occurs at that frequency in the NZ NO_5Oc and NZ O_5Oc structures instead couples with CH and NH twists, resulting in a distribution of weak bands. The calculated NZ NO_5Oc spectrum matches two of the experimental features but lacks a strong band at $\sim 1400\text{ cm}^{-1}$. The photodissociation intensity at $\sim 1000\text{ cm}^{-1}$ is consistent with a population of NZ O_5OOc , and NZ NO_5Oc structures may also be present and contribute to photodissociation in this region. All three of these structures, NZ O_5Oc , NZ O_5OOc , and NZ NO_5Oc , have similar calculated spectra and likely contribute to the observed spectrum.

$\text{Glu}\cdot\text{Ba}^{2+}$ and $\text{Glu}\cdot\text{Ca}^{2+}$. In the IR action spectra of both $\text{Glu}\cdot\text{Ba}^{2+}$ and $\text{Glu}\cdot\text{Ca}^{2+}$ (Figure 5), two bands are observed in the carbonyl stretch region centered at ~ 1600 and 1660 cm^{-1} and are attributed to the carbonyl stretches of a carboxylate and a carboxylic acid, respectively. The carboxylic acid carbonyl stretch is red-shifted from the corresponding band observed for H^+ , Li^+ , and Cs^+ , and this shift can be attributed to greater transfer of electron density to the divalent cation compared to the monovalent ions. The remaining features of the spectra are very similar to those observed in the IR action spectrum of $\text{Glu}\cdot\text{H}^+$: a broad band centered at $\sim 1440\text{ cm}^{-1}$ and three smaller bands at ~ 1290 , 1340 , and 1160 cm^{-1} . The experimental band at $\sim 1440\text{ cm}^{-1}$, corresponding to NH bends, is both higher in frequency and substantially broader than similar features observed in the IR action spectra of the lithiated and cesiated complexes. However, the width and frequency of this feature are similar to those observed in the protonated complexes, consistent with structures for both $\text{Glu}\cdot\text{Ba}^{2+}$ and $\text{Glu}\cdot\text{Ca}^{2+}$ that have a protonated N-terminus, providing additional evidence of zwitterionic structures.

A ZW O₅OO_C structure is calculated to be the most stable for both Glu•Ba²⁺ and Glu•Ca²⁺ (Table 2). Geometry optimization calculations were performed on a similar structure with a deprotonated side chain. However, no local minimum on the potential energy surface was found for this structure. The calculated spectra of the ZW O₅OO_C, NZ NO₅O_C, and NZ O₅O_C structures are all similar, but the measured frequencies of the two carbonyl bands are closest to those calculated for the ZW O₅OO_C structures. For Glu•Ca²⁺, the NZ NO₅O_C structure is calculated to be nearly isoenergetic with ZW O₅OO_C. However, both the frequencies of the carbonyl stretches and width of the NH bending bands near 1450 cm⁻¹ in the experimental spectrum are more consistent with the calculated spectrum of the ZW O₅OO_C structure. The NZ O₅O_C and ZW OO_C structures are at least 39 kJ/mol higher in energy than the ZW O₅OO_C structure for Glu•Ca²⁺ and at least 12 kJ/mol higher for Glu•Ba²⁺. The poor agreement with the measured spectra and these energies suggest that there is no significant contribution from ZW OO_C or NZ O₅O_C structures to the ion population.

Interestingly, the NZ O₅OO_C structure is not stable for these complexes. For Glu•Ca²⁺, this structure isomerizes to the similar, but zwitterionic, structure ZW O₅OO_C (Figure 5), during geometry optimization. For Glu•Ba²⁺, the ZW O₅OO_C structure does not converge nor does it isomerize during energy minimization, indicating the potential energy surface is very flat in this region.

Comparing Glu to Gln. The IR action spectra of Gln•M⁺ (M = Li, Cs), and Gln•Ba²⁺ were recently reported,^{13,14} and the structures of these complexes have essentially the same metal ion interactions with the amino acid as those determined for Glu. The spectra of the monocationized Gln complexes have two distinct carbonyl stretches separated by ~60 cm⁻¹. By comparison, FTIR absorption spectra of gas-phase acetic acid, acetamide, pentanoic acid, and pentanamide indicate that the intrinsic frequency of an amide carbonyl stretch is about 40–50 cm⁻¹ lower than the carbonyl stretch of the corresponding carboxylic acid.⁷² The carbonyl stretch of isolated alanine is at 1785 cm⁻¹,⁷³ ~10 cm⁻¹ higher than the corresponding band for propanoic acid.⁶⁰ These molecules should provide an indication of the intrinsic difference in carbonyl stretches of the C-terminus and side-chain carboxylic acid groups, respectively, in Glu. These results are consistent with the single, wide band in the IR action spectra of monocationized Glu. For Gln•Ba²⁺, bands at 1430, 1590, and 1650 cm⁻¹ are very similar in frequency and shape to those observed for Glu•Ba²⁺ and Glu•Ca²⁺, consistent with a similar structure for all three species.¹³

Glu is ~40 kJ/mol more acidic than Gln, and because they adopt similar structures in metal cationized complexes,^{13,63,64} the effects of gas-phase acidity on the stabilities of their zwitterionic structures can be directly compared. For Li⁺, the lowest-energy zwitterionic form is 32 and 33 kJ/mol higher in energy than the lowest-energy non-zwitterionic form for Glu and Gln, respectively. For Cs⁺, the zwitterionic form is calculated to be 4 kJ/mol more stable for both. Thus, the lower ΔH_{acid} of Glu compared to Gln has virtually no effect on the relative zwitterionic stabilities for these monocation complexes. The reason for this is that the metal cations prevent the side chain of Glu from interacting with the C-terminus and disrupt the interaction that is responsible for the high acidity of Glu.

In all the lowest-energy non-zwitterionic structures, the carbonyl oxygen of the side chain interacts directly with the metal ion. Results from Armentrout and co-workers show that the binding affinity of Na⁺ to Gln is 14 ± 1 kJ/mol higher than

to Glu.²⁰ For K⁺, this difference is 9 ± 1 kJ/mol.²¹ These results indicate that an amide group is more effective at stabilizing charge than a carboxylic acid group. This effect does not appear to be significant in preferentially stabilizing the non-zwitterionic form of Gln compared to Glu with either Li⁺ or Cs⁺.

For Ba²⁺, the lowest-energy zwitterionic structure is 17 and 2 kJ/mol more stable than the lowest-energy non-zwitterionic structure for Glu and Gln, respectively. In contrast to the results for the monovalent ions, the zwitterionic form is preferentially stabilized for Glu. The difference in the charge solvating ability of the amide vs the carboxylic acid should be greater for a dication than for a monocation due to greater transfer of electron density to the dication. For Li⁺ and Cs⁺, the lowest-energy zwitterionic structure is ZW OO_C, but for Ba²⁺, the ZW O₅OO_C in which the side chain coordinates directly to the divalent metal ion is most stable. Thus, the side-chain carbonyl oxygen interacts with Ba²⁺ in both the lowest-energy zwitterionic and non-zwitterionic forms of both Glu and Gln. The greater zwitterionic stability of Glu•Ba²⁺ compared to Gln•Ba²⁺ can be attributed to a greater relative stabilization of the non-zwitterionic structure of Gln•Ba²⁺ owing to effects of improved charge solvation by the amide vs the acid, rather than effects of intrinsic gas-phase acidity of the deprotonation site. This charge solvation effect may be lower for the zwitterionic form because there is transfer of electron density from the negatively charged carboxylate group to the metal dication, lowering the effective charge state of the metal ion.

Conclusions

Infrared photodissociation spectroscopy of mono- and divalent cations coordinated to Asp and Glu provides detailed structural information about the metal binding interaction to these two acidic amino acids. For the protonated, lithiated, and cesiated species, both amino acids are non-zwitterionic, whereas with Ca²⁺ and Ba²⁺, Glu is zwitterionic. On the basis of these results, Asp cationized with Ca²⁺ and Ba²⁺ is expected to be zwitterionic as well. The IR action spectra of the protonated species indicate spectral features associated with a protonated N-terminus and are useful for identifying potential zwitterionic structures for metal cationized species. The experimental spectra of both lithiated species are most consistent with an NZ NO₅O_C structure, whereas for the cesiated species, an NZ O₅OO_C and an NZ O₅O_C structure is adopted by Asp and Glu, respectively. The IR action spectra of Asp•M⁺ and Glu•M⁺ for each M investigated are very similar to each other, indicating that the longer side chain of Glu has only subtle effects on structure.

Cationized Gln has nearly the same metal ion interactions as does Glu and the relative stabilities of the non-zwitterionic and zwitterionic forms are nearly the same for both Li⁺ and Cs⁺, despite Glu being ~40 kJ/mol more acidic.^{63,64} For Glu•Ba²⁺, the relative stability of the zwitterionic form is 15 kJ/mol greater than that for Gln•Ba²⁺, due to the greater charge stabilization of the non-zwitterionic form by an amide vs a carboxylic acid group. These results indicate that the relative zwitterionic stability is not directly related to gas-phase acidity for these cationized amino acids.

Acknowledgment. IRMPD spectra were measured at the FOM Institute for Plasma Physics “Rijnhuizen”, which is financially supported by the Nederlandse Organisatie voor Wetenschappelijk Onderzoek (NWO), and we thank Dr. B. Redlich and the FELIX staff for excellent support. Generous financial support was provided by the National Science Foundation (Grants CHE-0718790 and OISE-730072).

Supporting Information Available: Full citation for ref 68. This material is available free of charge via the Internet at <http://pubs.acs.org>.

References and Notes

- Bellissent-Funel, M. C. *J. Mol. Liq.* **2000**, *84*, 39–52.
- Hofmeister, F. *Arch. Exp. Pathol. Pharmacol.* **1888**, *24*, 247–260.
- Para, G.; Jarek, E.; Warszynski, P. *Adv. Colloid Interface Sci.* **2006**, *122*, 39–55.
- Thomas, A. S.; Elcock, A. H. *J. Am. Chem. Soc.* **2007**, *129*, 14887–14898.
- Zhou, H. X. *Proteins: Struct., Funct., Bioinf.* **2005**, *61*, 69–78.
- Rodgers, M. T.; Armentrout, P. B. *Acc. Chem. Res.* **2004**, *37*, 989–998.
- Rodgers, M. T.; Armentrout, P. B. *J. Am. Chem. Soc.* **2000**, *122*, 8548–8558.
- Kaltashov, I. A.; Zhang, M. X.; Eyles, S. J.; Abzalimov, R. R. *Anal. Bioanal. Chem.* **2006**, *386*, 472–481.
- Veenstra, T. D. *Biophys. Chem.* **1999**, *79*, 63–79.
- Ruan, C. H.; Rodgers, M. T. *J. Am. Chem. Soc.* **2004**, *126*, 14600–14610.
- Bush, M. F.; O'Brien, J. T.; Prell, J. S.; Saykally, R. J.; Williams, E. R. *J. Am. Chem. Soc.* **2007**, *129*, 1612–1622.
- Armentrout, P. B.; Rodgers, M. T.; Oomens, J.; Steill, J. D. *J. Phys. Chem. A* **2008**, *112*, 2248–2257.
- Bush, M. F.; Oomens, J.; Saykally, R. J.; Williams, E. R. *J. Phys. Chem. A* **2008**, doi: 10.1021/ja803121w.
- Bush, M. F.; Oomens, J.; Saykally, R. J.; Williams, E. R. *J. Am. Chem. Soc.* **2008**, *130*, 6463–6471.
- Bush, M. F.; Prell, J. S.; Saykally, R. J.; Williams, E. R. *J. Am. Chem. Soc.* **2007**, *129*, 13544–13553.
- Dunbar, R. C.; Polfer, N. C.; Oomens, J. *J. Am. Chem. Soc.* **2007**, *129*, 14562–14563.
- Forbes, M. W.; Bush, M. F.; Polfer, N. C.; Oomens, J.; Dunbar, R. C.; Williams, E. R.; Jockusch, R. A. *J. Phys. Chem. A* **2007**, *111*, 11759–11770.
- Kamariotis, A.; Boyarkin, O. V.; Mercier, S. R.; Beck, R. D.; Bush, M. F.; Williams, E. R.; Rizzo, T. R. *J. Am. Chem. Soc.* **2006**, *128*, 905–916.
- Kapota, C.; Lemaire, J.; Maitre, P.; Ohanessian, G. *J. Am. Chem. Soc.* **2004**, *126*, 1836–1842.
- Heaton, A. L.; Moision, R. M.; Armentrout, P. B. *J. Phys. Chem. A* **2008**, *112*, 3319–3327.
- Heaton, A. L.; Armentrout, P. B. *J. Phys. Chem. B* **2008**, *112*, 12056–12065.
- Jockusch, R. A.; Lemoff, A. S.; Williams, E. R. *J. Am. Chem. Soc.* **2001**, *123*, 12255–12265.
- Wytenbach, T.; Witt, M.; Bowers, M. T. *J. Am. Chem. Soc.* **2000**, *122*, 3458–3464.
- Lemoff, A. S.; Bush, M. F.; Williams, E. R. *J. Am. Chem. Soc.* **2003**, *125*, 13576–13584.
- Lemoff, A. S.; Bush, M. F.; O'Brien, J. T.; Williams, E. R. *J. Phys. Chem. A* **2006**, *110*, 8433–8442.
- Talley, J. M.; Cerda, B. A.; Ohanessian, G.; Wesdemiotis, C. *Chem.-Eur. J.* **2002**, *8*, 1377–1388.
- Lemoff, A. S.; Bush, M. F.; Williams, E. R. *J. Phys. Chem. A* **2005**, *109*, 1903–1910.
- Bush, M. F.; Forbes, M. W.; Jockusch, R. A.; Oomens, J.; Polfer, N. C.; Saykally, R. J.; Williams, E. R. *J. Phys. Chem. A* **2007**, *111*, 7753–7760.
- Polfer, N. C.; Oomens, J.; Dunbar, R. C. *Phys. Chem. Chem. Phys.* **2006**, *8*, 2744–2751.
- Rodgers, M. T.; Armentrout, P. B.; Oomens, J.; Steill, J. D. *J. Phys. Chem. A* **2008**, *112*, 2258–2267.
- Polfer, N. C.; Oomens, J.; Moore, D. T.; von Helden, G.; Meijer, G.; Dunbar, R. C. *J. Am. Chem. Soc.* **2006**, *128*, 517–525.
- Strittmatter, E. F.; Lemoff, A. S.; Williams, E. R. *J. Phys. Chem. A* **2000**, *104*, 9793–9796.
- Oh, H.; Breuker, K.; Sze, S. K.; Ge, Y.; Carpenter, B. K.; McLafferty, F. W. *Proc. Natl. Acad. Sci. U.S.A.* **2002**, *99*, 15863–15868.
- Oh, H. B.; Lin, C.; Hwang, H. Y.; Zhai, H. L.; Breuker, K.; Zabrouskov, V.; Carpenter, B. K.; McLafferty, F. W. *J. Am. Chem. Soc.* **2005**, *127*, 4076–4083.
- Rajabi, K.; Fridgen, T. D. *J. Phys. Chem. A* **2008**, *112*, 23–30.
- Baker, E. S.; Manard, M. J.; Gidden, J.; Bowers, M. T. *J. Phys. Chem. B* **2005**, *109*, 4808–4810.
- Barran, P. E.; Polfer, N. C.; Campopiano, D. J.; Clarke, D. J.; Langridge-Smith, P. R. R.; Langley, R. J.; Govan, J. R. W.; Maxwell, A.; Dorin, J. R.; Millar, R. P.; Bowers, M. T. *Int. J. Mass Spectrom.* **2005**, *240*, 273–284.
- Baker, E. S.; Gidden, J.; Ferzoco, A.; Bowers, M. T. *Phys. Chem. Chem. Phys.* **2004**, *6*, 2786–2795.
- Stearns, J. A.; Mercier, S.; Seaiby, C.; Guidi, M.; Boyarkin, O. V.; Rizzo, T. R. *J. Am. Chem. Soc.* **2007**, *129*, 11814–11820.
- Stearns, J. A.; Guidi, M.; Boyarkin, O. V.; Rizzo, T. R. *J. Chem. Phys.* **2007**, *127*, 154322.
- Polfer, N. C.; Oomens, J.; Dunbar, R. C. *ChemPhysChem* **2008**, *9*, 579–589.
- Kong, X. L.; Tsai, I. A.; Sabu, S.; Han, C. C.; Lee, Y. T.; Chang, H. C.; Tu, S. Y.; Kung, A. H.; Wu, C. C. *Angew. Chem., Int. Ed.* **2006**, *45*, 4130–4134.
- Simon, A.; MacAleese, L.; Maitre, P.; Lemaire, J.; McMahon, T. B. *J. Am. Chem. Soc.* **2007**, *129*, 2829–2840.
- Wu, R.; McMahon, T. B. *J. Mass Spectrom.* **2008**, doi: 10.1002/jms.1449.
- Wu, R. H.; McMahon, T. B. *J. Am. Chem. Soc.* **2007**, *129*, 4864–4865.
- Wytenbach, T.; Witt, M.; Bowers, M. T. *Int. J. Mass Spectrom.* **1999**, *182–183*, 243–252.
- Lemoff, A. S.; Wu, C. C.; Bush, M. F.; Williams, E. R. *J. Phys. Chem. A* **2006**, *110*, 3662–3669.
- Lemoff, A. S.; Williams, E. R. *J. Am. Soc. Mass Spectrom.* **2004**, *15*, 1014–1024.
- Jockusch, R. A.; Lemoff, A. S.; Williams, E. R. *J. Phys. Chem. A* **2001**, *105*, 10929–10942.
- Jockusch, R. A.; Price, W. D.; Williams, E. R. *J. Phys. Chem. A* **1999**, *103*, 9266–9274.
- Ai, H. Q.; Bu, Y. X.; Han, K. L. *J. Chem. Phys.* **2003**, *118*, 10973–10985.
- Hoyau, S.; Ohanessian, G. *Chem.-Eur. J.* **1998**, *4*, 1561–1569.
- Hoyau, S.; Pelicier, J. P.; Rogalewicz, F.; Hoppilliard, Y.; Ohanessian, G. *Eur. J. Mass Spectrom.* **2001**, *7*, 303–311.
- Remko, M.; Rode, B. M. *J. Phys. Chem. A* **2006**, *110*, 1960–1967.
- Belcastro, M.; Marino, T.; Russo, N.; Toscano, M. *J. Mass Spectrom.* **2005**, *40*, 300–306.
- Constantino, E.; Rodriguez-Santiago, L.; Sodupe, M.; Tortajada, J. *J. Phys. Chem. A* **2005**, *109*, 224–230.
- Ling, S. L.; Yu, W. B.; Huang, Z. J.; Lin, Z. J.; Haranczyk, M.; Gutowski, M. *J. Phys. Chem. A* **2006**, *110*, 12282–12291.
- Julian, R. R.; Beauchamp, J. L.; Goddard, W. A. *J. Phys. Chem. A* **2002**, *106*, 32–34.
- Rak, J.; Skurski, P.; Simons, J.; Gutowski, M. *J. Am. Chem. Soc.* **2001**, *123*, 11695–11707.
- Strittmatter, E. F.; Williams, E. R. *Int. J. Mass Spectrom.* **2001**, *212*, 287–300.
- Strittmatter, E. F.; Wong, R. L.; Williams, E. R. *J. Phys. Chem. A* **2000**, *104*, 10271–10279.
- Hunter, E. P. L.; Lias, S. G. *J. Phys. Chem. Ref. Data* **1998**, *27*, 413–656.
- Jones, C. M.; Bernier, M.; Carson, E.; Colyer, K. E.; Metz, R.; Pawlow, A.; Wischow, E. D.; Webb, I.; Andriole, E. J.; Poutsma, J. C. *Int. J. Mass Spectrom.* **2007**, *267*, 54–62.
- Li, Z.; Matus, M. H.; Velazquez, H. A.; Dixon, D. A.; Cassady, C. J. *Int. J. Mass Spectrom.* **2007**, *265*, 213–223.
- Caldwell, G.; Renneboog, R.; Kebarle, P. *Can. J. Chem.* **1989**, *67*, 611–618.
- Valle, J. J.; Eyley, J. R.; Oomens, J.; Moore, D. T.; van der Meer, A. F. G.; von Helden, G.; Meijer, G.; Hendrickson, C. L.; Marshall, A. G.; Blakney, G. T. *Rev. Sci. Instrum.* **2005**, *76*, 023103.
- Oepts, D.; Vandermeer, A. F. G.; Vanamersfoort, P. W. *Infrared Phys. Technol.* **1995**, *36*, 297–308.
- Shao, Y.; et al. *Phys. Chem. Chem. Phys.* **2006**, *8*, 3172–3191.
- Ross, R. B.; Powers, J. M.; Atashroo, T.; Ermler, W. C.; Lajohn, L. A.; Christiansen, P. A. *J. Chem. Phys.* **1990**, *93*, 6654–6670.
- Oomens, J.; Sartakov, B. G.; Meijer, G.; Von Helden, G. *Int. J. Mass Spectrom.* **2006**, *254*, 1–19.
- Oomens, J.; van Roij, A. J. A.; Meijer, G.; von Helden, G. *Astrophys. J.* **2000**, *542*, 404–410.
- FTIR spectra obtained from NIST Webbook. URL: <http://webbook.nist.gov/chemistry/>.
- Linder, R.; Seefeld, K.; Vavra, A.; Kleinermaans, K. *Chem. Phys. Lett.* **2008**, *453*, 1–6.